sciendo

DOI: 10.2478/eces-2024-0001 ECOL CHEM ENG S. 2024;31(1):7-17

Korumilli TARANGINI[1], Shilo Nesa SHERLIN[1], Shanuja JAKKALA[1]
Pallbhika BORAH[1], Stanisław WACŁAWEK[2], Sankarannair SABARINATH[3]
Korukonda Jagajjanani RAO[1*] and Vinod V.T. PADIL[3*]

OPTIMISING BIOSYNTHESIS OF ANTIMICROBIAL COPPER NANOPARTICLES USING AQUEOUS *Aegle marmelos* LEAF EXTRACT-BASED MEDIUM

Abstract: Copper oxide nanostructures have garnered significant attention in nanotechnology for their diverse applications. This study presents a green synthesis approach using an aqueous *Aegle marmelos* leaf extract-based medium to produce copper oxide (Cu_4O_3) nanoparticles. Optimisation was achieved through a simplified Taguchi L9 orthogonal array, investigating critical parameters such as temperature, surfactants (AOT and Tween 80), and additives (ascorbic acid and chitosan). Under optimised conditions (AOT: 0.0012 mM, ascorbic acid: 10 mM, chitosan: 1 %, temperature: 80 °C), near-spherical nanoparticles of ~200 nm were obtained. Comprehensive characterisation through UV-Vis, DLS, electron microscopy, XRD, and FTIR spectroscopy confirmed the nanoparticles' properties, while antibacterial assays showed promising results against *Escherichia coli* bacteria.

Keywords: green synthesis, copper oxide, Taguchi method, *Aegle marmelos*, antimicrobial properties

Introduction

Nanobiotechnology, an exciting fusion of nanotechnology and biotechnology, has emerged as a novel field where nanoparticles are synthesised through biological entities [1]. The unique properties of nanoparticles, stemming from their extremely small size and large surface area to volume ratio, play a pivotal role in various domains, including optics, electronics, imaging, biomedicine, and bioscience [2]. Among metallic nanoparticles, copper nanoparticles (CuNPs) have garnered significant attention in recent times due to their desirable characteristics [3]. Notably, CuNPs have found extensive use in wound dressing applications, owing to their potential as biocidal, antibacterial, antifungal, and healing agents [3, 4]. The ease of availability, cost-effectiveness, and resemblance to noble metal properties further amplify the interest in CuNPs [3, 5].

CuNPs can be synthesised through diverse methods, such as precipitation, bioreduction, laser ablation, sol-gel processes, chemical vapor deposition, electrochemical

[1] Department of Biotechnology, Centre for Interfaces & Nanomaterials, C/O Research Park, Vel Tech Rangarajan Dr. Sagunthala R&D Institute of Science and Technology, Chennai-600062, India, ORCID: KJR 0000-0002-9592-7655
[2] Institute for Nanomaterials, Advanced Technologies and Innovation, Technical University of Liberec, Studentská 1402/2, 46117, Liberec 1, Czech Republic, ORCID: 0000-0002-8430-8269
[3] Amrita School for Sustainable Futures (ASF), Amrita Vishwa Vidyapeetham, Amrita University, Amritapuri, Kollam, Kerala, India, ORCID: VVTP 0000-0002-0816-526X
[*] Corresponding authors: drjagajjananirao@veltech.edu.in, vinodvtp@am.amrita.edu

deposition, hydrothermal techniques, and certain biological approaches [6]. Among these, the reduction of respective metal salts by sodium borohydride followed by functionalisation with surfactants, stabilising agents, or polymeric ligands is a prevalent technique for nanoparticle synthesis [6]. However, the green synthesis route, involving bioresources like plants, has gained traction due to its eco-friendliness [3, 5]. These green approaches offer safer and cleaner routes for producing nanoparticles with a wide range of sizes, shapes, structures, compositions, and physicochemical properties [3, 5, 7]. Recent reports have showcased the synthesis of CuNPs using various plant extracts, presenting diverse applications. For instance, the use of *Justicia adhatoda* leaf extract for antibacterial coatings [8], *Manilkara zapota* leaf extract with photocatalytic, antiproliferative and antimicrobial properties [9], strawberry fruit extract for incorporating cytotoxicity, antioxidant and cutaneous wound healing [10], *Abies spectabilis* plant extract with antinociceptive and anti-inflammatory potential [11], *Madhuca longifolia* plant extract for wastewater treatment [12] and *Celastrus paniculatus* leaf extract for photocatalytic and antifungal properties [13]. The resulting CuNPs from the stated studies are predominantly composed of CuO, often with spherical and near-spherical shapes and varying size ranges.

CuNPs have a long history of application in treating microbial infections due to their potent toxicity against a broad spectrum of microbes, including fungi and bacteria [8, 14]. Their large surface area contributes to enhanced antimicrobial action by facilitating effective electrostatic binding and conjugation with biological systems. However, synthesising nanoparticles with homogeneous sizes and shapes typically involves complex multi-step procedures, high-temperature treatments, usage of corrosive or toxic chemicals, and separate stabilisation compounds, making the process intricate [15-17]. Overcoming the challenges of dealing with multiple parameters calls for the utilisation of statistical design methodologies like Taguchi's approach, which saves time and reduces chemical wastage [18, 19]. The Taguchi approach employs orthogonal arrays to optimise all design parameters and minimise variation with the fewest possible experiments, simplifying the optimisation process [18, 19]. Scaling up the nanoparticle synthesis process to produce small-sized particles remains a challenge as they tend to agglomerate and follow polydispersity during synthesis [18, 19]. Optimisation of parameters becomes imperative for achieving nanoparticles with smaller sizes.

In this study, we meticulously investigated the formation of CuNPs in an aqueous medium using *A. marmelos* leaf extract. The selection of *A. marmelos* leaf extract was based on its richness in polyphenolic compounds, particularly tannins, known for their properties as reducing and stabilising agents [17, 20, 21]. Previous studies from our group reported their ability to reduce silver and gold salts [17, 20, 21]. The Taguchi approach was employed to determine the conditions for controlling size and polydispersity, focusing on crucial parameters such as surfactant (AOT/Tween 80), ascorbic acid, chitosan, and temperature. To ensure safe synthesis, non-toxic surfactants (AOT/Tween 80) [22] and additives (ascorbic acid and chitosan) were chosen for CuNPs stabilisation [18, 19]. The combination of surfactants controlling nanoparticle size and the reducing and stabilising properties of ascorbic acid and chitosan, in addition to *A. marmelos* leaf extract, proved effective for CuNPs synthesis [16, 23]. The role of temperature influencing nanoparticle synthesis was also investigated as a parameter in this study. The optimised conditions yielded CuNPs with high stability, narrow size distribution, and a well-defined surface plasmon resonance (SPR) band around 435 nm. These CuNPs, of paramelaconite

Cu_4O_3 type, displayed promising antimicrobial activity against *E. coli* bacteria, further highlighting their potential for biomedical applications.

Materials and methods

Primarily, fresh leaves of *A. marmelos* were used to make aqueous plant extract and a stock of 5 % leaf extract solution was prepared as per our reported study with minor modifications [17]. In brief, 5 g of dried leaf powder is added to 100 mL of double distilled water and this mixture was heated to 100 °C on a hot plate for 10 min with continuous shaking using a magnetic stirrer. The resultant extract was subjected to centrifugation (8000 rpm for 15 min) and filtration (using a filter disc of pore size 0.45 µm). Then, the extract was further freeze-dried using CareBiosDFD-10 Laboratory Freeze Dryer, China and converted to a powder form which was used for further investigation.

Table 1

Parameters selected for Taguchi method with their levels for the synthesis of CuNPs

S.No.	Parameters/Factors	Level 1	Level 2	Level 3
1	Surfactant	AOT	Tween 80	None
2	Ascorbic acid [mM]	None	5	10
3	Chitosan [%]	None	1	2
4	Temperature [°C]	Room temperature	50	80

*AOT and Tween used are of 0.0012 mM and 2.5 mM which are their individual critical micelle concentration values.

All chemicals were prepared in aqueous media. For the synthesis of CuNPs, copper(I) acetate (100 mM) was prepared. For process acceleration and optimisation of key synthesis parameters; additives (ascorbic acid and chitosan) and surfactants (AOT, Tween 80) were selected. Chitosan solution (5 %) was prepared using 1 % acetic acid whereas ascorbic acid (50 mM) was prepared and used as additives. Surfactants, AOT (15 mM) and Tween 80 (125 mM) stock solutions were also prepared for process optimisation studies.

Experimental design, optimisation and statistical analysis were performed as follows: metal salt/leaf extract (1 mM/0.5 %) in an aqueous medium was identified to produce CuNPs at ambient conditions at a slower rate (72 h - 96 h) with larger sizes of 1 µm to 5 µm (Fig. S1). To limit the time of synthesis and to have control on size distribution; the influence of additives and surfactants was studied further. With a constant ratio of metal salt/leaf extract (1 mM/0.5 %); optimisation of four factors i.e. surfactant, ascorbic acid, chitosan and temperature (Table 1) were studied in three levels using Taguchi approach for CuNPs synthesis. The levels of Table 1 are selected from our previous experimental results (data not shown here). Taguchi L9 array with different trials was investigated, as shown in Table 2. Here, the reaction time for each experiment was allowed to proceed for 120 min. And UV-Vis absorption maximum (A_{max}) values from CuNPs formation due to SPR were evaluated (Fig. 1).

Based on the tabulated primary results (Table 2), a verification test was done to check the optimum condition for CuNPs synthesis (with a higher A_{max} value) and analysis of variance (ANOVA) for the obtained results was also performed to identify the key factors affecting the synthesis approach. For the experimental design, ANOVA calculation and the optimisation strategy, MNITAB® Release 14 (Minitab Inc, USA) was used. Furthermore,

analysis, characterisation and antimicrobial assay was given in supplementary information (ESI).

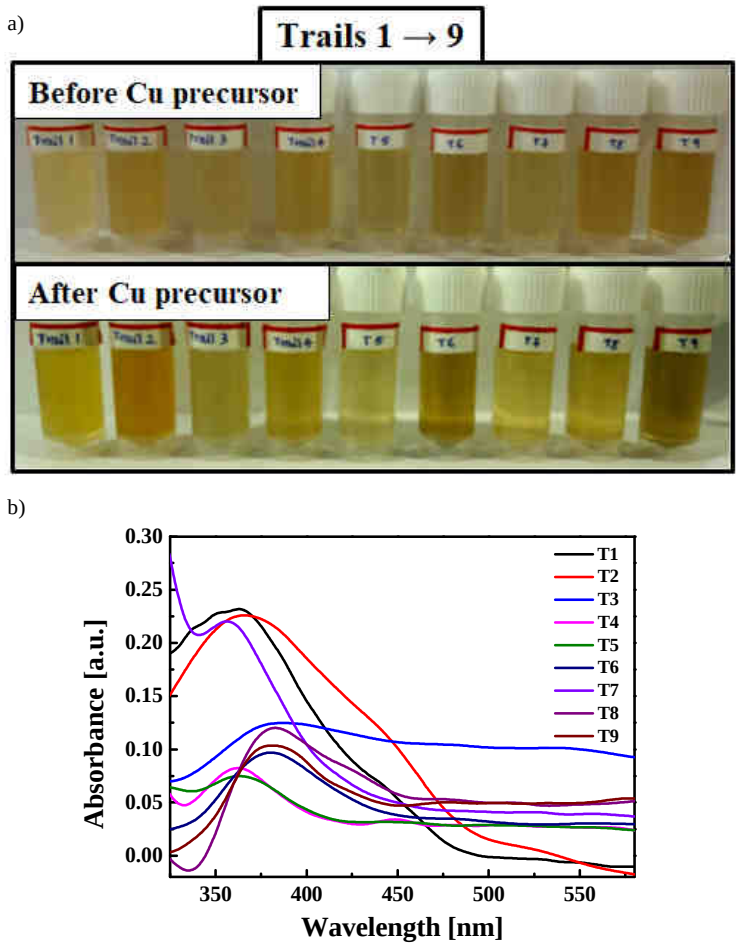


Fig. 1. a) Colour changes in samples due to the formation of CuNPs in 9 experimental trials; b) UV-Vis spectral analysis of the experimental trials with absorption maximum (A_{max}) of each stated trail after ~4 times dilution

Results and discussion

The synthesis of CuNPs and the Taguchi optimisation of process parameters are the key steps in this study. Synthesis and stabilisation of nanoparticles through wet chemical methods are challenging as there will be multiple parameters to control the selective size and dimensions of nanostructures [18, 19]. Taguchi's approach will help in achieving homogenous particle suspensions by fine-tuning of various factors with limited experimentation. Recent studies displayed its effectiveness in size and shape control of inorganic nanoparticles and the Taguchi design has the advantage of including continuous

and categorical factors [17]. Our group has reported the synthesis of size and shape control of Ag and Au nanoparticles using Taguchi optimisation methodology employing *A. marmelos* with various additives [17]. However, the synthesis of CuNPs and deducing the best procedural conditions were explored using the Taguchi approach and attempted in this study. Reports state that stabilising agents like surfactants and additives are influential in CuNPs synthesis [24], and these are studied along with temperature using a simple L9 experimental array of the Taguchi method (Table 2).

The colour changes in the media before, and after the addition of metal precursor is shown in Figure 1a and their UV-Vis spectral signatures due to SPR are given in Figure 1b. In general, nanoparticles interact with light and effectively block light at specific wavelengths from passing, thus exhibiting distinctive colour. The colour effect depends on the plasmon resonance; the higher the absorption intensity, the more the SPR effect, which is a physical phenomenon useful in sensor fabrication and new-generation optics [25]. Thus, maximum absorption intensity values (A_{max}) are significant in indicating fewer aggregation states [17]. So, CuNPs with more A_{max} values are of interest and our process design tabulated these values from each trail in Table 2. From the Table, trail 1 exhibited an A_{max} value of 0.233 which is higher than the other combinations studied.

Table 2

Experimental conditions and results for CuNPs synthesis under varying factors with metal salt/leaf extract ratio of 1 mM/0.5 %, AOT (0.0012 mM) and Tween 80 (2.5 mM). Except trials 3, 4, 8; all other trials were exposed to sonication for 2 h and RT indicates room temperature (30 °C)

Trials	Surfactant	Ascorbic acid [mM]	Chitosan [%]	Temperature [°C]	A_{max} (values from 330 nm to 550 nm)
1	AOT	10	1	50	0.233
2	AOT	5	2	80	0.226
3	AOT	0	0	RT	0.125
4	Tween 80	10	2	RT	0.084
5	Tween 80	5	0	50	0.076
6	Tween 80	0	1	80	0.098
7	None	10	0	80	0.222
8	None	5	1	RT	0.072
9	None	0	2	50	0.105

Table 3

Analysis of variance (ANOVA) of main effects of factors studied

Factor	DF	Seq SS	Adj SS	Adj MS	F	P
Surfactant	2	0.0178	0.0178	0.0089	74.98	0.013
Ascorbic acid	2	0.0074	0.0074	0.0037	31.27	0.031
Temperature	2	0.0079	0.0079	0.0039	33.46	0.029
Residual Error	2	0.0002	0.0002	0.0001		
Total	8	0.0335				

DF - degree of freedom; Seq SS - the sequential sum of squares; Adj SS - adjusted sums of squares; Adj MS - adjusted mean squares; F - value is the ratio of variation between the group and within the group; P - probability value

The main effects of factors are studied to observe the maximum influence of individual factor on the output (i.e., CuNPs with more A_{max} value). Figure 2 shows the average value of the observed results each at its individual A_{max} value obtained from 9 experiments (Table

2). The horizontal line in each smaller graph of Figure 2 corresponds to the overall average A_{max} value of Table 2 for the respective factor studied. ANOVA results for the synthesis of CuNPs are shown in Table 3. Here, change in 'surfactant' was considered as the most significant parameter (with a *p*-value of 0.013, significant at the 0.05 α-level), then followed by 'temperature' (with a *p*-value of 0.029) and 'ascorbic acid' (with a *p*-value of 0.031). The parameters with *p*-values > 0.1 generally have the least importance on the synthesis approach and are ignored.

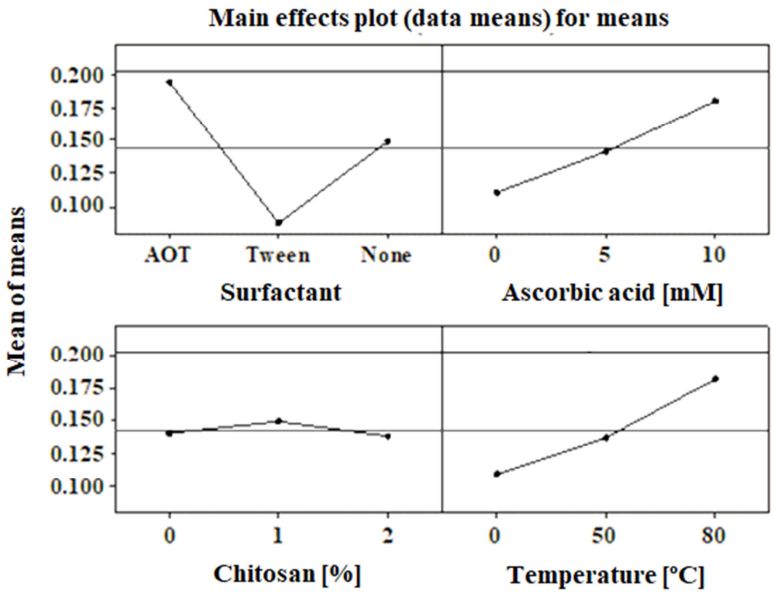


Fig. 2. Main effects of factors or the average of obtained results in which each factor is at a given level, as shown in Table 2

Table 4

Optimum synthesis conditions suggested by statistical calculations after performing the tests

Parameter	Level description	Level	Contribution (A_{max} value)
Surfactant	AOT	1	0.194
Ascorbic acid [mM]	10	3	0.179
Chitosan [%]	1	2	0.150
Temperature [°C]	80	3	0.182
Total contribution of all (compared to the average value)			0.133
Average value			0.143
Expected result at optimum condition			0.276

After assessing the results, the optimum conditions for the synthesis of CuNPs, which are optically active with intense A_{max} value are estimated by statistical calculations and summarised in Table 4. From the table values, the estimated SPR absorption intensity is 0.276 for CuNPs with optimum conditions. A trial experiment was performed using the stated optimum conditions (Fig. 3) and the experimental result of ~0.305 at 435 nm

(Fig. 3a) was observed. This value is very close to that of the predicted value of ~0.276 (Table 4), which is ~2.2 times more than the value of the maximum average intensity of CuNPs (Table 2). The observed experimental A_{max} value (Fig. 3a) from optimum conditions is ~10 % more than the predicted value, and the difference between the predicted and actual result is minimal and acceptable. In addition to the above, the estimated linear model analysis (Table S1) of means with R_2 values > 99 % indicates that our regression model fits the data well.

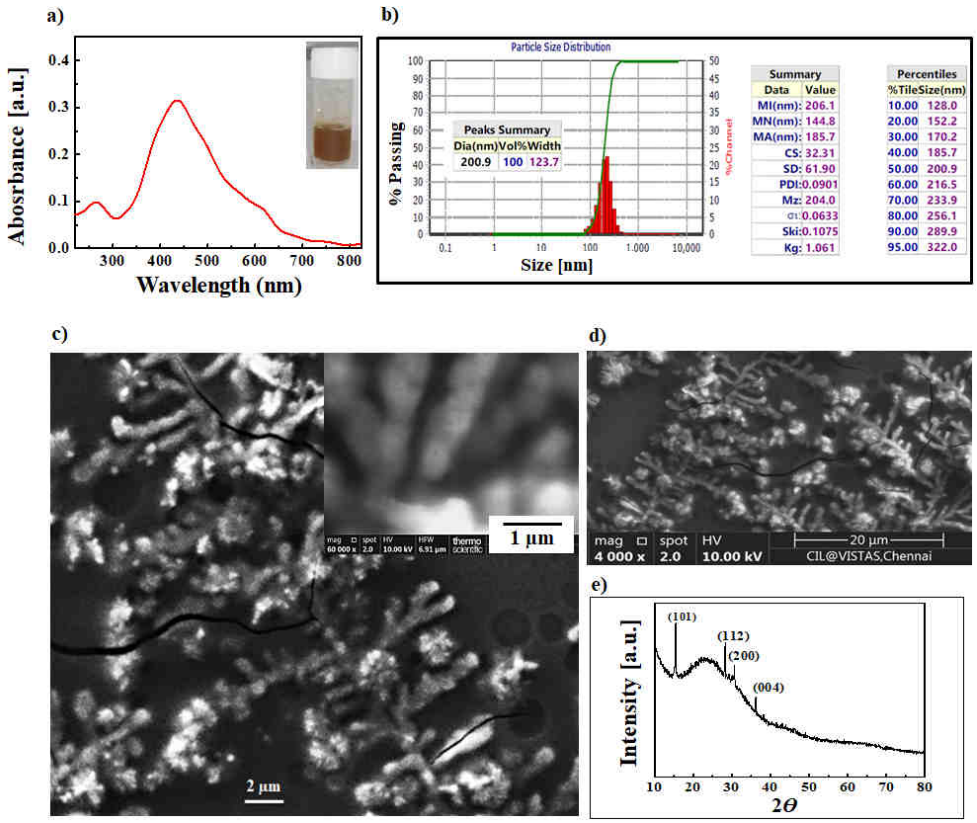


Fig. 3. a) UV-Vis spectrum of CuNPs from optimised parameters, b) DLS size measurements, c) and d) corresponds to SEM analysis, e) XRD pattern of the synthesised particles

Figure 3a shows the SPR spectral pattern with Amax at 435 nm of CuNPs from the optimised reaction conditions and the colour change of the solution shown in the picture insert. Particle size analysis (Fig. 3b) indicates monodispersity and the average diameter of CuNPs was observed to be ~200 nm. The size and morphology were further confirmed by SEM analysis (Fig. 3c,d), where the CuNPs suspension drop dried on a silicon wafer for analysis. Here, CuNPs are self-assembled and formed branched structures where particles from each branch in close-up are shown in Figure 3c insert. A low-magnification image (Fig. 3d) shows its spreadability throughout the surface upon drying. This pattern is expected as the prepared CuNPs has chitosan, AOT and ascorbic acid, which, on drying,

tends to form network structures [26, 27]. A detailed analysis and study regarding self-assembly is going on and not discussed in this study. The crystallinity of CuNPs was confirmed by XRD pattern of Figure 3e where prominent diffraction pattern with peaks (101), (112), (200), and (004) matches with a tetragonal system of Cu_4O_3 with JCPDS Card No. 33-0480 and also matches with reported study as well [28]. Furthermore, while surfactant and ascorbic acid influence is negligible, a diffraction pattern with chitosan was also seen in Figure 3e which corresponds to its amorphous nature and matches with JCPDS Card No. 39-1894 [29].

CuNPs from optimum synthesis parameters upon repeated water washings (three) were analysed by FTIR spectroscopy (Fig. 4a). The Figure shows significant peaks at 3285 cm^{-1} (O-H stretch from the phenolic groups or chitosan), 2883 cm^{-1} (C-H stretching in the aromatic compound or chitosan), 1576 cm^{-1} (for C=C), 1375 cm^{-1} (for OH group), 1149 cm^{-1} (for C-O stretch), 1070 cm^{-1} and 1025 cm^{-1} (for C-O stretch of phenol) along with a small peak at 888 cm^{-1} region (for C-H out of plane bend). These observations indicate that these peaks are from characteristic aromatic phenols like tannins, as reported in our previous study using *A. marmelos* leaf extract [20]. Moreover, though the amine peak of chitosan around 3380 cm^{-1} merged with *A. marmelos* leaf extract's O-H peak, its typical presence was seen with a peak at ~1650 cm^{-1}[30]. Additionally, the band at ~1325 cm^{-1} is from stretching vibrations of C-O group of chitosan [31]. The absence of a relatively dominant band at 1095 cm^{-1} from -C-O-C- group of chitosan states that it could be involved in bonding with tannins [32]. With the above inferences, we can say CuNPs are majorly stabilised with phenolic compounds, tannin and chitosan participation in particle capping and stabilisation. Furthermore, the other ingredients of the medium, AOT and ascorbic acid are absent in the washed CuNPs surface and not influential in stabilisation. FTIR spectrums of individual components are given in Figure S2 of ESI.

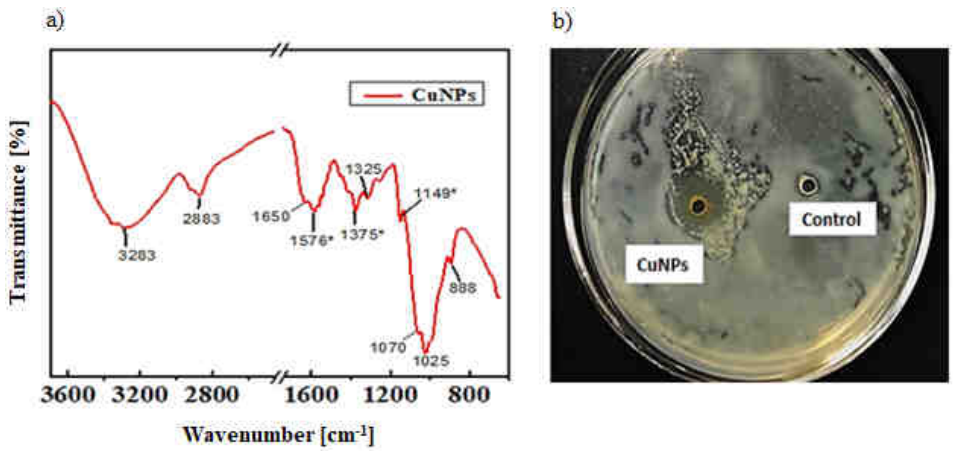


Fig. 4. a) FTIR analysis of CuNPs produced from optimised process conditions using *A. marmelos* medium and their b) Antimicrobial activity against *E. coli*. Control in (b) corresponds to medium devoid of CuNPs

The antimicrobial property of CuNPs was tested against *E. coli* (Fig. 4b). The NA plate with *E. coli* displayed ZOI value of 8.94 mm ±2.13 mm with CuNPs in the well while there

is no significant ZOI was observed with the control well devoid of CuNPs and comprise of only reaction components [*A. marmelos* leaf extract (0.5 %), AOT (0.0012 mM), ascorbic acid (10 mM), chitosan (1 %)]. In general, copper in its Cu_4O_3 (paramelaconite) phase existence is rare and difficult to synthesise in comparison with other phases like CuO (tenorite) and Cu_2O (cuprite). The metastable Cu_4O_3 with 1.33 copper to oxygen atom ratio is reported to possess decent antimicrobial action [28] and multimodal action by Cu_4O_3 was observed by various researchers with diverse mechanisms. These include the production of reactive oxygen species, membrane leakage, cell death due to Cu^{2+} ions release and interaction with sulfhydral groups inside cell membrane were reported [28, 33, 34]. Further, as reported previously, the large surface area of these nanoparticles can also enhance their antimicrobial activity [35]. In complementary to the reported evidence, our results through plate studies state that the synthesised CuNPs are efficient, and the observations are confirmed with three replicate investigations. Our result is in the match with a reported study with similar ZOI values reported when *Cicer arietinum* extract was employed for the synthesis of CuNPs of Cu_4O_3 type [28]. Thus, these particles have a huge scope for use in healthcare, biomedical and environmental fields. Facile synthesis of CuNPs in this study through green chemicals and by optimisation of process parameters makes the approach environmentally benign, saves time and could be promising for large-scale production.

Conclusion

In conclusion, achieving precise size and shape control of nanostructures through green synthesis poses challenges, and exploring various process parameters can be a laborious task. However, employing the Taguchi approach in statistical process design proves advantageous, saving time and minimising the wastage of valuable chemicals. This study demonstrates a straightforward Taguchi optimisation method to synthesise homogeneous CuNPs in a short timeframe, utilising an aqueous *A. marmelos* leaf extract-based medium with additives (AOT, ascorbic acid, and chitosan). XRD analysis confirms the crystal system of CuNPs as tetragonal, specifically of paramelaconite (Cu_4O_3) type, while FTIR analysis verifies the *in situ* stabilisation of the formed nanoparticles. Additionally, the ZOI assay validates the antimicrobial properties of CuNPs against *E. coli*. This approach proposes a large-scale synthesis of antimicrobial CuNPs, readily applicable in the fields of biomedical and nanotechnology.

Acknowledgements

The authors would like to thank the Vel Tech Rangarajan Dr.Sagunthala R&D Institute of Science and Technology, India, for providing laboratory facilities during the project's execution. The authors (Vinod V.T. Padil and Sabarinath S.) gratefully acknowledge the Amrita Seed fund (Ref. ASG2022104) grant for the project titled '*Porous 2D Membranes and 3D Sponges Based on Sustainable Functionalised Bio-gum/MXene nanocomposites for the detection and removal of microplastics' by Amrita Vishwa Vidyapeetham and* support provided by Amrita School for sustainable Futures, Amrita Vishwa Vidyapeetham, Amritapuri campus, Kollam, Kerala, India.

References

[1] Talebpour F, Ghahghaei A. Effect of green synthesis of gold nanoparticles (AuNPs) from Hibiscus sabdariffa on the aggregation of α-lactalbumin. Int J Pept Res Ther. 2020;26(4):2297-306. DOI: 10.1007/s10989-020-10023-9.

[2] Kamala Nalini SP, Vijayaraghavan K. Green synthesis of silver and gold nanoparticles using aloe vera gel and determining its antimicrobial properties on nanoparticle impregnated cotton fabric. J Nanotechnol Res. 2020;2(3):42-50. Available from: https://www.fortunejournals.com/articles/green-synthesis-of-silver-and-gold-nanoparticles-using-aloe-vera-gel-and-determining-its-antimicrobial-properties-on-nanoparticle-.html.

[3] Ansari N, Lodha A, Patel TL. A novel microwave-assisted green synthesis of copper nanoparticles using Citrus limon and its application for antibacterial and antifungal activity. Int J Nanosci. 2022;21(3):2250016. DOI: 10.1142/S0219581X22500168.

[4] Mohan VR, Doss A, Tresina PS, Beulah GGP, Juliet MR. Biogenic synthesis of copper nanoparticles using aquatic pteridophyte Marsilea quadrifolia Linn. rhizome and its antibacterial activity. Int J Nano Dimension. 2020;11(4):337-45. Available from: https://journals.iau.ir/article_674921.html.

[5] Umer A, Naveed S, Ramzan N, Rafique MS, Imran M. A green method for the synthesis of copper nanoparticles using L-ascorbic acid. Matéria. 2014;19(3):197-203. DOI: 10.1590/S1517-70762014000300002.

[6] Naz S, Gul A, Zia M. Toxicity of copper oxide nanoparticles: a review study. IET Nanobiotechnol. 2019;14(1):1-13. DOI: 10.1049/iet-nbt.2019.0176.

[7] Sharma D, Kanchi S, Bisetty K. Biogenic synthesis of nanoparticles: A review. Arabian J Chem. 2019;12(8):3576-600. DOI: 10.1016/j.arabjc.2015.11.002.

[8] Md. Islam J, Khatun MT, Md. Rahman R, Alam MM. Green synthesis of copper oxide nanoparticles using Justicia adhatoda leaf extract and its application in cotton fibers as antibacterial coatings. AIP Adv. 2021;11(12):125223. DOI: 10.1063/5.0076941.

[9] Kiriyanthan RM, Sharmili SA, Balaji R, Jayashree S, Mahboob S, Al-Ghanim KA, et al. Photocatalytic, antiproliferative and antimicrobial properties of copper nanoparticles synthesized using Manilkara zapota leaf extract: A photodynamic approach. Photodiagnosis Photodyn Ther. 2020;32:102058. DOI: 10.1016/j.pdpdt.2020.102058.

[10] Hemmati S, Ahmeda A, Salehabadi Y, Zangeneh A, Zangeneh MM. Synthesis, characterization, and evaluation of cytotoxicity, antioxidant, antifungal, antibacterial, and cutaneous wound healing effects of copper nanoparticles using the aqueous extract of strawberry fruit and l-ascorbic acid. Polyhedron. 2020;144:25180. DOI: 10.1016/j.poly.2020.114425.

[11] Liu H, Zheng S, Xiong H, Alwahibi MS, Niu X. Biosynthesis of copperoxide nanoparticles using Abies spectabilis plant extract and analyzing its antinociceptive and anti-inflammatory potency in various mice models. Arabian J Chem. 2020;139:6995-7006. DOI: 10.1016/j.arabjc.2020.07.006.

[12] Das P, Ghosh S, Ghosh R, Dam S, Baskey M. Madhuca longifolia plant mediated green synthesis of cupric oxide nanoparticles: A promising environmentally sustainable material for waste water treatment and efficient antibacterial agent. J Photochem Photobiol B: Biology. 2018;189:66-73. DOI: 10.1016/j.jphotobiol.2018.09.023.

[13] Mali SC, Dhaka A, Githala CK, Trivedi R. Green synthesis of copper nanoparticles using Celastrus paniculatus Willd. leaf extract and their photocatalytic and antifungal properties. Biotechnol Rep (Amst). 2020;27:e00518. DOI: 10.1016/j.btre.2020.e00518.

[14] Dankovich TA, Smith JA. Incorporation of copper nanoparticles into paper for point-of-use water purification. Water Res. 2014;63:245-51. DOI: 10.1016/j.watres.2014.06.022.

[15] Rao KJ, Paria S. Phytochemicals mediated synthesis of multifunctional Ag-Au-TiO_2 heterostructure for photocatalytic and antimicrobial applications. J Cleaner Prod. 2017;165:360-8. DOI: 10.1016/j.jclepro.2017.07.147.

[16] Rao KJ, Paria S. Mixed phytochemicals mediated synthesis of multifunctional Ag-Au-Pd nanoparticles for glucose oxidation and antimicrobial applications. ACS Appl Mater Interfaces. 2015;7(25):14018-25. DOI: 10.1021/acsami.5b03089.

[17] Rao KJ, Paria S. Aegle marmelos leaf extract and plant surfactants mediated green synthesis of Au and Ag nanoparticles by optimizing process parameters using Taguchi method. ACS Sust Chem Eng. 2015. DOI: 10.1021/acssuschemeng.5b00022.

[18] Akyalcin S, Akyalcin L, Bjørgen M. Optimization of desilication parameters of low-silica ZSM-12 by Taguchi method. Microporous Mesoporous Materials. 2019;273:256-64. DOI: 10.1016/j.micromeso.2018.07.014.

[19] Rao KJ, Korumilli T, Jakkala S, Singh K, Vidya K. Optimization of the one-step green synthesis of silver and gold nanoparticles using aqueous Athyrium filix femina extract using the Taguchi method. BioNanoScience. 2021;11(4):915-22. DOI: 10.1007/s12668-021-00909-3.
[20] Rao KJ, Paria S. Green synthesis of silver nanoparticles from aqueous Aegle marmelos leaf extract. Materials Res Bull. 2013;48(2):628-34. DOI: 10.1016/j.materresbull.2012.11.035.
[21] Rao KJ, Paria S. Green synthesis of gold nanoparticles using aqueous Aegle marmelos leaf extract and its application for thiamine detection. RSC Adv. 2014; 28645-52. DOI: 10.1039/C4RA03883E.
[22] Othumpangat S, Fedan JS. Oil spills. In: Reference Module in Biomedical Sciences, Elsevier. 2022. DOI: 10.1016/B978-0-12-824315-2.00166-4.
[23] Phan TTV, Hoang G, Nguyen VT, Nguyen TP, Kim HH, Mondal S, et al. Chitosan as a stabilizer and size-control agent for synthesis of porous flower-shaped palladium nanoparticles and their applications on photo-based therapies. Carbohydrate Polymers. 2019;205:340-52. DOI: 10.1016/j.carbpol.2018.10.062.
[24] Dang TMD, Le TTT, Fribourg-Blanc E, Dang MC. The influence of solvents and surfactants on the preparation of copper nanoparticles by a chemical reduction method. Adv Nat Sci: Nanosci Nanotechnol. 2011;2(2):025004. DOI: 10.1088/2043-6262/2/2/025004.
[25] Takemura K. Surface plasmon resonance (SPR)- and localized SPR (LSPR)-based virus sensing systems: optical vibration of nano- and micro-metallic materials for the development of next-generation virus detection technology. Biosensors. 2021;11(8):8. DOI: 10.3390/bios11080250.
[26] Singh KG, Singh G, Kang TS. Aggregation behavior of sodium dioctyl sulfosuccinate in deep eutectic solvents and their mixtures with water: An account of solvent's polarity, cohesiveness, and solvent structure. ACS Omega. 2018;3(10):13387-98. DOI: 10.1021/acsomega.8b01637.
[27] Nocelli NE, de las Zulueta Díaz YM, Millot M, Colazo ML, Vico RV, Fanani ML. Self-assembled nanostructures of L-ascorbic acid alkyl esters support monomeric amphotericin B. Heliyon. 2021;7(1):e06056. DOI: 10.1016/j.heliyon.2021.e06056.
[28] Thanuja J, Udayabhanu, Nagaraju G, Naika HR. Biosynthesis of Cu_4O_3 nanoparticles using Razma seeds: application to antibacterial and cytotoxicity activities. SN Appl Sci. 2019;1(12):1646. DOI: 10.1007/s42452-019-1556-3.
[29] Ali MAE, Aboelfadl MMS, Selim AM, Khalil HF, Elkady GM. Chitosan nanoparticles extracted from shrimp shells, application for removal of Fe(II) and Mn(II) from aqueous phases. Separation Sci Technol. 2018;53(18):2870-81. DOI: 10.1080/01496395.2018.1489845.
[30] Drabczyk A, Kudłacik-Kramarczyk S, Głąb M, Kędzierska M, Jaromin A, Mierzwiński D, et al. Physicochemical investigations of chitosan-based hydrogels containing Aloe vera designed for biomedical use. Materials. 2020;13(14):3073. DOI: 10.3390/ma13143073.
[31] Machodi MJ, Daramol MO. Synthesis and performance evaluation of PES/chitosan membranes coated with polyamide for acid mine drainage treatment. Sci Rep. 2019;9(1):1. DOI: 10.1038/s41598-019-53512-8.
[32] Sionkowska A, Kaczmarek B, Lewandowska K. Characterisation of chitosan after cross-linking by tannic acid. PCACD. 2014;19(1);135-8. DOI: 10.15259/PCACD.19.16.
[33] Mittapally S, Taranum R, Parveen S. Metal ions as antibacterial agents. J Drug Delivery Ther. 2018;8(6):411-9. DOI: 10.22270/jddt.v8i6-s.2063.
[34] Mohammadi Ziarani G, Khademi M, Mohajer F, Badiei A, Varma RS. The synthesis of 2,2-bis(1-indol-3-yl)acenaphthylene-1(2)-ones using nanocatalysis: Fluorescent sensing for Cu^{2+} ions. Ecol Chem Eng S. 2022;29(4):463-75. DOI: 10.2478/eces-2022-0033.
[35] Narath S, Shankar SS, Sivan SK, George B, Thomas TD, Sabarinath S, et al. Facile green synthesis of Cinnamomum tamala extract capped silver nanoparticles and its biological applications. Ecol Chem Eng S. 2023;30(1):7-21. DOI: 10.2478/eces-2023-0001.